*Turbulence, Heat and Mass Transfer 4, pp. 401–408*
*K. Hanjalić, Y. Nagano and M. Tummers (Editors)*


# DNS in a Plane vertical Channel With and Without Buoyancy

Lars Davidson[1], Dalibor Čuturić[1] and Shia-Hui Peng[2]

[1] *Dept. of Thermo and Fluid Dynamics, Chalmers University of Technology, SE-412 96 Göteborg, Sweden, http://www.tfd.chalmers.se/~lada*

[2] *FOI (Swedish Defence Research Agency), Aeronautics Division, SE-172 90 Stockholm*

**Abstract** — DNS of fluid flow and heat transfer is presented for fully developed flow in a vertical channel at $Re_\tau = 150$. Both forced convection and mixed convection ($Gr = 7.68 \cdot 10^6$) are studied. Mean flow and second-moment quantities such as stresses and heat fluxes are presented. In forced convection, away from the viscous dominated layers, the shear stress term in the momentum equation balances the pressure gradient. However, in mixed convection the buoyancy term plays a major role which strongly modifies the shear stress, which is increased near the cold wall and reduced near the hot wall. As a result all stresses are affected in the same way. Surprisingly, the effect of buoyancy on temperature fluctuations $\overline{t^2}$ is vice versa. The reason for this behaviour is given in the paper.
It is shown that the effect of buoyancy on the turbulence takes place in the momentum equation. The buoyancy terms in the stress equations are negligible. It is concluded that Reynolds stress models should be used for buoyancy-affected flows, not because an accurate modeling of the effect of buoyancy in the Reynolds stress equations is needed, but because no direct stress-strain coupling is assumed.

## 1. Equations

The equations have the form

$$\frac{\partial U_i}{\partial x_i} = 0 \tag{1}$$

$$\frac{\partial U_i}{\partial t} + \frac{\partial}{\partial x_j}(U_i U_j) = \delta_{i1} - \frac{1}{\rho}\frac{\partial P}{\partial x_i} + \frac{1}{Re_\tau}\frac{\partial^2 U_i}{\partial x_j \partial x_j} + \frac{Gr}{Re_\tau^2}(T - T_{ref})\delta_{1i} \tag{2}$$

$$\frac{\partial T}{\partial t} + \frac{\partial}{\partial x_j}(U_j T) = \frac{1}{Pr Re_\tau}\frac{\partial^2 T}{\partial x_j \partial x_j} \tag{3}$$

The Reynolds number $Re_\tau = u_\tau h/\nu = 150$ is based on the friction velocity, $u_\tau$ (related to the driving pressure gradient $\delta_{i1}$), and the half channel width, $h$ ($h = \rho = u_\tau = 1$ so that $\nu = 1/Re_\tau$). All quantities in Eqs. 1-3 are made non-dimensional with $u_\tau$, $h$ and $\Delta T$ and $T_{ref} \equiv 0.5(T_{hot} + T_{cold}) = 0.5$. The temperature at the left boundary ($y = 0$) is $T = 1$ (hot wall) and at the right wall $T = 0$, see Fig. 1a.

The streamwise, wall-normal and spanwise directions are denoted by $x$ ($x_1$), $y$ ($x_2$) and $z$ ($x_3$) respectively. Periodic boundary conditions were applied in the $x$ and $z$ direction (homogeneous directions).

## 2. Numerical Method

An incompressible, finite volume code is used [1]. For space discretization, second-order central differencing is used for all terms. The second-order Crank-Nicolson scheme is used for time discretization. The numerical procedure is based on an implicit, fractional step technique with a multigrid pressure Poisson solver and a non-staggered grid arrangement [2].

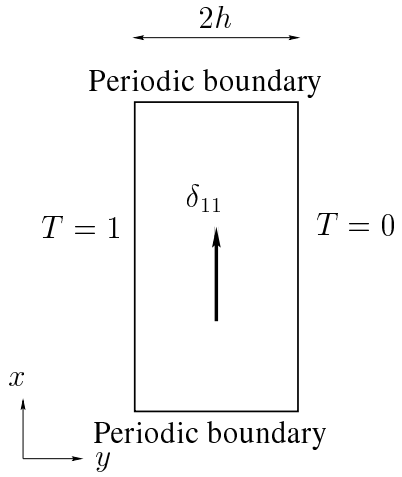


(a) Configuration.

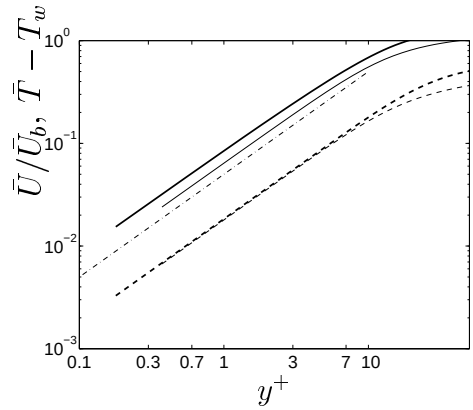


(b) Thin lines: $Gr = 0$; thick lines: $Gr = 7.68 \cdot 10^6$. Solid lines: $\bar{U}/\bar{U}_b$; dashed lines: $\bar{T}$; dash-dotted line: *const.* $y^+$.

Figure 1: Configuration and near-wall behaviour of mean profiles (left, hot wall).

| | $\tau_{w,y=0}$ | $\tau_{w,y=2h}$ | $x_{max}$ | $\bar{U}_b$ | $u_*$ | $\Delta y^+_{node,min}$ | $(\partial\bar{T}/\partial y)_w$ |
|---|---|---|---|---|---|---|---|
| $Gr = 0$ | 1 | 1 | $4\pi$ | 15.6 | 1 | 0.4 | 2.69 |
| $Gr = 0$ (DNS [3]) | 1 | 1 | $5\pi$ | 15.2 | 1 | - | 2.54 |
| $Gr = 7.68 \cdot 10^6$ | 0.708 | 0.419 | $8\pi$ | 9.8 | 0.75 | 0.2 | 2.31 |

Table 1: Mesh details and global physical quantities. $z_{max} = \pi$ for both cases. $u_* = \left[0.5\left((u_*^2)^{left} + (u_*^2)^{right}\right)\right]^{1/2}$.

## 3. Results

For the forced convection a grid with $64 \times 64 \times 64$ cells is used and for the mixed convection a mesh with $128 \times 96 \times 96$ $(x, y, z)$ cells. For more details, see Table 1.

For the mixed convection case it was found that a very large box size in the vertical direction $(8\pi)$ was needed. If a smaller box was used no quasi-steady conditions were obtained, but the bulk velocity varied with a very low frequency [4]. Figure 2 presents the mean velocity and temperature profiles as well as the normal stresses for the two cases. For the forced convection case the DNS results from Ref. [3] are also included. The agreement between the present results and the DNS results is fairly good.

For the forced convection case, all quantities in Fig. 2 are symmetric whereas for the mixed convection case they are non-symmetric. In order to study the effect of buoyancy on the flow, we start by taking a closer look at the momentum equation. Equation 2 is turned into Reynolds equations using Reynolds decomposition $U = \bar{U} + u$. Integrating the one-dimensional Reynolds equation for $\bar{U}$ from $y = 0$ to $y$ we get

$$0 = y - \overline{uv}\Big|_y + \nu \frac{\partial \bar{U}}{\partial y}\Big|_y - \tau_w + \underbrace{\frac{Gr}{Re_\tau^2}\int_0^y (\bar{T} - \bar{T}_{ref})dy'}_{B} \tag{4}$$

where the terms represent the prescribed driving pressure gradient, the turbulent shear stress at

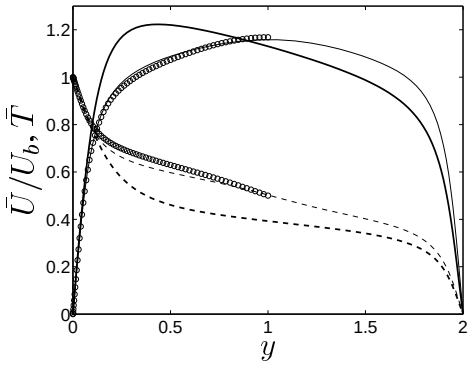


(a) Solid lines: $\bar{U}/U_b$; dashed lines: $\bar{T}$.

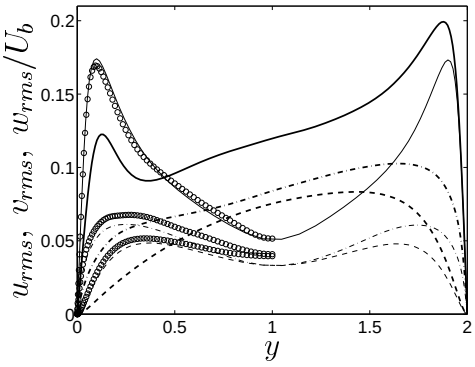


(b) Solid lines: $\overline{u^2}$; dashed lines: $\overline{v^2}$; dash-dotted lines: $\overline{w^2}$.

Figure 2: Mean flow and RMS velocities. Thin lines: $Gr = 0$; thick lines: $Gr = 7.68 \cdot 10^6$. Markers denote DNS from Ref. [3].

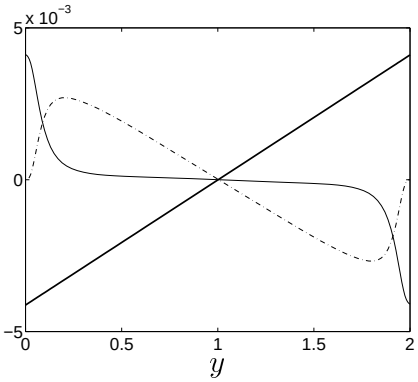


(a) $Gr = 0$.

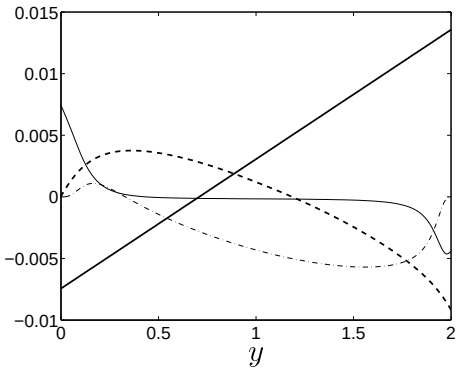


(b) $Gr = 7.68 \cdot 10^6$.

Figure 3: The terms in the integrated $\bar{U}$ momentum equation (Eq. 4). All terms are scaled by $U_b^2$. Thick solid line: driving pressure gradient plus $\tau_w$; thin solid line: viscous shear stress; dash-dotted line: turbulent shear stress; thick dashed line: buoyancy term $B$.

$y$, the viscous shear stress at $y$ and at the wall, and the buoyancy force, respectively. The terms in the $\bar{U}$-equation are shown in Fig. 3. For the forced convection we have the usual balance between viscous and turbulent shear stress and the pressure gradient. For the mixed convection case, the buoyancy term is aiding the flow in the left half of the channel, and it is opposing in the right half. In Fig. 3 it can be seen that the buoyancy term is positive in the left part and negative in the right part. Since the temperature profile is not symmetric, the buoyancy term is not zero at $y = 1$. The velocity profile is also asymmetric, and the wall shear stress at the left wall ($\tau_w^{left} = \rho(u_*^2)^{left}$) is different from that on the right wall ($\tau_w^{right} = \rho(u_*^2)^{right}$). This is also seen in Fig. 3 where the magnitude of the viscous shear stress at the walls are equal for the forced convection case but not for the mixed convection case. Contrary to the forced convection case, the wall shear stresses are not balanced by the pressure gradient, but they are balanced by the sum of the pressure gradient and the buoyancy force. Hence $\tau_w = \rho u_*^2 = 0.5(\tau_w^{left} + \tau_w^{right}) \neq 1$

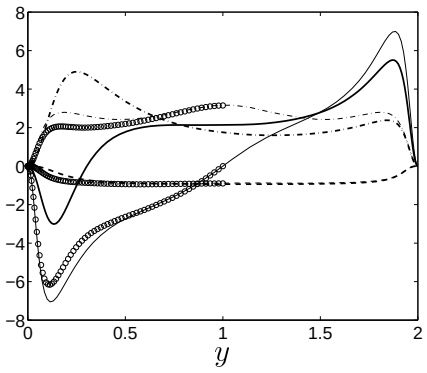


(a) Solid lines: $\overline{ut}/|q_w|$; dashed lines: $-\overline{vt}/|q_w|$; dash-dotted lines: $500\overline{t^2}$. Markers denote DNS from Ref. [3].

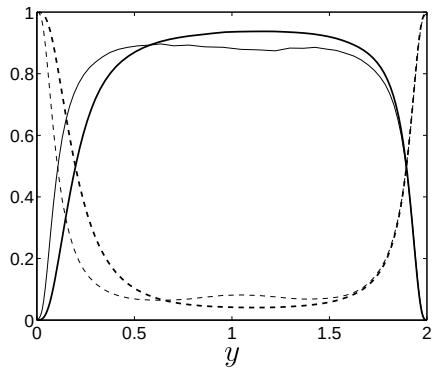


(b) Solid lines: turbulent heat flux $\overline{vt}/|q_w|$; dashed lines: viscous heat flux $-1/(Re_\tau\, Pr|q_w|)\partial\bar{T}/\partial y$.

Figure 4: Temperature related quantities. Thin lines: $Gr = 0$; thick lines: $Gr = 7.68 \cdot 10^6$.

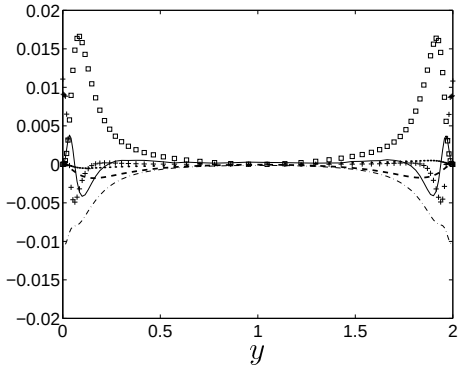


(a) $Gr = 0$.

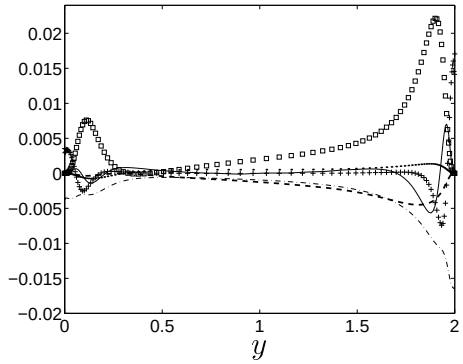


(b) $Gr = 7.68 \cdot 10^6$.

Figure 5: Balance for the $\overline{u^2}$ equation. All terms scaled by $U_b^3$. Solid line: $D_{uu}^T$; thick dashed line: $\Pi_{uu}$; dash-dotted line: $\varepsilon_{uu}$; $+$ : $D_{uu}^\nu$; $\square$ : $P_{uu}$; $\cdot$ : $G_{uu}$.

(see Table 1). Also, it can be seen that whereas in the forced convection case, the turbulent shear stress is linear in the region where viscous effects are negligible this is not the case for the mixed convection case. The turbulent shear stress $-\overline{uv}$ is strongly modified when buoyancy is introduced, and its magnitude compared with the forced convection case is increased near the right, cold wall and decreased near the left, hot wall, see Fig. 3. As a results all normal stresses are affected in the same way, see Fig. 2b.

Note that the velocity in all figures have been scaled with the bulk velocity. The reason is that both $u_*$ and the bulk Reynolds number for the mixed convection case is much lower than for the forced convection case, see Table 1. An alternative would be to use $u_*$ for normalizing, which would give a 20% relative decrease in the velocities for the mixed convection case compared to the chosen normalization. We should, however, keep in mind that as we approach pure natural convection, we should include the wall heat flux as a scaling parameter [5].

Figure 1b presents the near-wall behaviour of the mean velocity and temperature. It can be

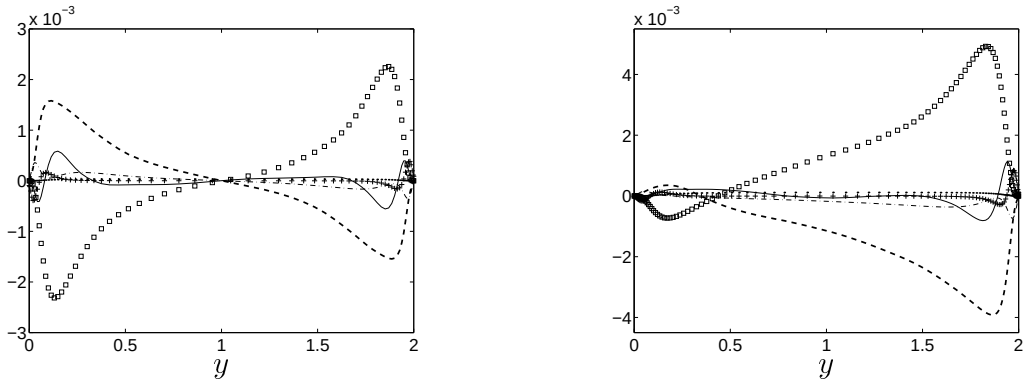


(a) $Gr = 0$. (b) $Gr = 7.68 \cdot 10^6$.

Figure 6: Balance for the $\overline{uv}$ equation. All terms scaled by $U_b^3$. Solid line: $D_{uv}^T$; thick dashed line: $\Pi_{uv}$; dash-dotted line: $\varepsilon_{uv}$; $+$ : $D_{uv}^\nu$; $\square$ : $P_{uv}$; $\cdot$ : $G_{uv}$.

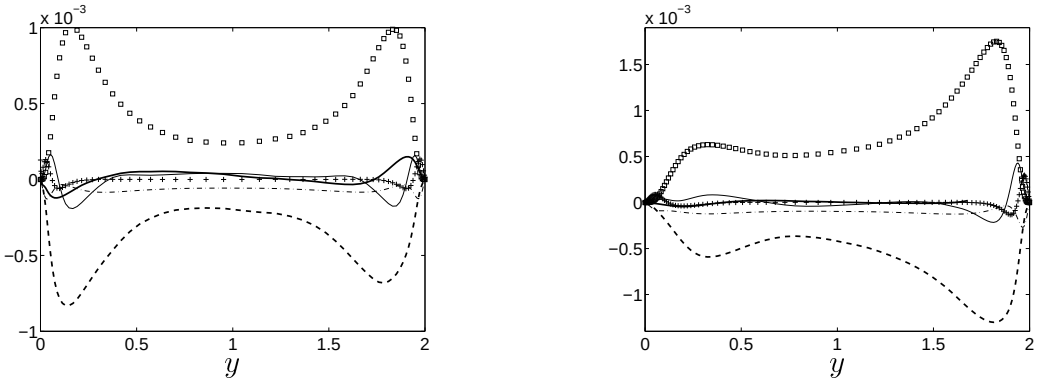


(a) $Gr = 0$. (b) $Gr = 7.68 \cdot 10^6$.

Figure 7: Balance for the $\overline{vt}$ equation. All terms scaled by $U_b^2$. Solid line: $D_{vt}^T$; dashed line: $\Pi_{vt}$; dash-dotted line: $\varepsilon_{vt}$; $+$ : $D_{vt}^\nu$; $\square$ : $P_{vt}$.

seen that there is a distinct linear region, both for $\bar{U}$ and $\bar{T}$, up to at least $y^+ = 5$. In the experimental investigation of a natural convection boundary layer in [6], it was found that the linear region for the velocity was very small (smaller than one viscous unit).

The overall balance of the $\bar{T}$ equation (Eq. 3) dictates that the total heat flux

$$q \equiv q_w = 1/(Re_\tau Pr)\partial\bar{T}/\partial y - \overline{vt} \tag{5}$$

must be independent of the wall-normal coordinate $y$. It can be seen from Fig. 2 that the $\bar{T}$ profile is not modified by buoyancy as much as the velocity profile. The reason is, of course, that there is no buoyancy term in the temperature equation. Since the turbulence in the mixed convection case is reduced near the left wall compared to the forced convection case, a larger part of the heat flux $q$ in Eq. 5 must near the left wall be taken care of by viscous transport (conduction) in the former case. This is illustrated in Fig. 2 where it is seen that the temperature gradient near the left wall is larger for the mixed convection case than in the forced convection case. Also Fig. 4b shows that the viscous transport near the left, hot wall is larger for $Gr =$

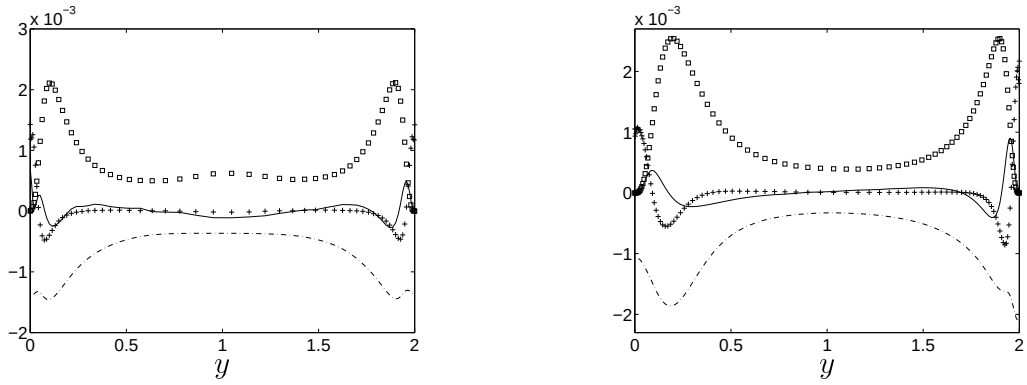


(a) $Gr = 0$. (b) $Gr = 7.68 \cdot 10^6$.

Figure 8: Balance for the $\overline{t^2}$ equation. All terms scaled by $U_b$. Solid line: $D^T_{tt}$; dash-dotted line: $\varepsilon_{tt}$; $+$ : $D^\nu_{tt}$; $\square$ : $P_{tt}$.

$7.68 \cdot 10^6$ than for $Gr = 0$.

### 3.1. Analysis of balances of the second moments

The transport equations for $\overline{u^2}$ and $\overline{uv}$ read

$$
\begin{aligned}
0 &= \underbrace{-2\overline{uv}\frac{\partial \bar{U}}{\partial y}}_{P_{uu}} \underbrace{-\frac{2}{\rho}u\frac{\overline{\partial p}}{\partial y}}_{\Pi_{uu}} \underbrace{-\frac{\partial \overline{u^2 v}}{\partial y}}_{D^T_{uu}} + \underbrace{\frac{1}{Re_\tau}\frac{\partial^2 \overline{u^2}}{\partial y^2}}_{D^\nu_{uu}} \underbrace{-\frac{2}{Re_\tau}\overline{\frac{\partial u}{\partial x_k}\frac{\partial u}{\partial x_k}}}_{\varepsilon_{uu}} + \underbrace{2\frac{Gr}{Re_\tau^2}\overline{ut}}_{G_{uu}} \\
0 &= \underbrace{-\overline{v^2}\frac{\partial \bar{U}}{\partial y}}_{P_{uv}} \underbrace{-\frac{1}{\rho}u\frac{\overline{\partial p}}{\partial y} - \frac{1}{\rho}v\frac{\overline{\partial p}}{\partial x}}_{\Pi_{uv}} \underbrace{-\frac{\partial \overline{uv^2}}{\partial y}}_{D^T_{uv}} + \underbrace{\frac{1}{Re_\tau}\frac{\partial^2 \overline{uv}}{\partial y^2}}_{D^\nu_{uv}} \underbrace{-\frac{2}{Re_\tau}\overline{\frac{\partial u}{\partial x_k}\frac{\partial v}{\partial x_k}}}_{\varepsilon_{uv}} + \underbrace{\frac{Gr}{Re_\tau^2}\overline{vt}}_{G_{uv}}
\end{aligned}
\tag{6}
$$

where the terms represent production ($P_{uu}$, $P_{uv}$), velocity-pressure gradient ($\Pi_{uu}$, $\Pi_{uv}$), turbulent diffusion by velocity correlations ($D^T_{uu}$, $D^T_{uv}$), viscous diffusion ($D^\nu_{uu}$, $D^\nu_{uv}$), dissipation ($\varepsilon_{uu}$, $\varepsilon_{uv}$) and buoyancy ($G_{uu}$, $G_{uv}$), respectively.

The transport equation for $\overline{vt}$ reads

$$
0 = \underbrace{-\overline{v^2}\frac{\partial \bar{T}}{\partial y}}_{P_{vt}} \underbrace{-\overline{\frac{t}{\rho}\frac{\partial p}{\partial y}}}_{\Pi_{vt}} \underbrace{-\frac{\partial \overline{v^2 t}}{\partial y}}_{D^T_{vt}} + \underbrace{\frac{1}{Re_\tau Pr}\frac{\partial}{\partial y}v\overline{\frac{\partial t}{\partial y}} + \frac{1}{Re_\tau}\frac{\partial}{\partial y}t\overline{\frac{\partial v}{\partial y}}}_{D^\nu_{vt}} \underbrace{-\left(\frac{1}{Re_\tau} + \frac{1}{Re_\tau Pr}\right)\overline{\frac{\partial v}{\partial x_k}\frac{\partial t}{\partial x_k}}}_{\varepsilon_{vt}}
\tag{7}
$$

It should again be noted that in order to facilitate comparison between the forced and mixed convection flows all terms in the balance equations have been normalized by the bulk velocity. As mentioned above the shear stress profile in Fig. 3 is strongly modified for the mixed convection flow compared to the forced convection flow. In the former case $|\overline{uv}|$ is reduced near the left, hot wall and it is increased along the right, cold wall. This gives, via $P_{uu}$ (Eq. 6 and Fig. 5), a large $\overline{u^2}$ near the right, cold wall. As a result $\overline{v^2}$ and $\overline{w^2}$ are also increased via the pressure-strain term. As $\overline{v^2}$ increases near the right wall, this also increases the production of

$\overline{uv}$ via $P_{uv}$ (see Eq. 6 and Fig. 6), which gives a large $|\overline{uv}|$. Thus we have a positive feedback mechanism between $\overline{uv}$, $\overline{u^2}$, and $\overline{v^2}$.

Note that the buoyancy term in the balance equations for $\overline{u^2}$ and $\overline{uv}$ is negligible. It is also negligible in the $\overline{v^2}$ and $\overline{w^2}$ equations (not shown). The effect of buoyancy enters the Reynolds stress equations via the balance of the momentum equation which modifies the shear stress and via the production and the pressure-strain affects the other stresses. Thus, modeling of the buoyancy terms in the Reynolds stress equations is only of minor importance. However, looking at the shear stresses and the velocity gradients in Figs. 2a and 3 it is immediately realized that there is no coupling between these two quantities. Thus, the only type of model which can predict buoyancy-affected flow is Reynolds stress models, and the reason is not an accurate modeling of the effect of buoyancy in the Reynolds stress equations, but the fact that no direct stress-strain coupling is assumed.

Above, the effect of buoyancy was discussed starting by looking at the momentum equation and its balance (Eq. 4 and Fig. 3). In the same way, before discussing the balance of the heat flux equations, let us start with the mean temperature equation and its balance (Eq. 5). The terms are shown in Fig. 4b and it can be seen that for the mixed convection case the magnitude of the wall-normal heat flux, $|\overline{vt}|$, decreases near the left, hot wall compared to the forced convection case. Near the right, cold wall there is no difference in $|\overline{vt}|$ for the two cases. Near the hot wall, the viscous heat flux, i.e. the mean temperature gradient, must increase for the mixed convection case in order to satisfy Eq. 5. This acts so as to increase $|\overline{vt}|$ via $P_{vt}$ in Eq. 7, but since this would violate Eq. 5, $\overline{v^2}$ must be suppressed, and the result is actually that $P_{vt}$ is decreased, see Fig. 7. Here we have a negative feedback between $\partial\bar{T}/\partial y$, $\overline{vt}$ and $\overline{v^2}$.

The wall-normal heat flux is only affected indirectly by the buoyancy compared with the stresses. The reason is of course that $\overline{vt}$ is the dominating term in Eq. 5, and this equation must be satisfied. The streamwise heat flux $|\overline{ut}|$, however, is affected similarly to the stresses (Fig. 4a). For the mixed convection case it is large near the right, cold wall because its production terms $-\overline{v^2}\partial\bar{T}/\partial y$ and $-\overline{vt}\partial\bar{U}/\partial y$ are both positive and large. However, contrary to the stresses, it is not larger than for the forced convection case. It is seen that there is no link between the heat flux $\overline{vt}$ and the temperature gradient $\partial\bar{T}/\partial y$ and thus eddy-viscosity models are unable to predict the forced convection case; also for the heat fluxes the direct effect of buoyancy in the heat flux equations is negligible.

All stresses as well as the streamwise heat flux are for the mixed convection case larger near the right wall than near the left wall, and the wall-normal heat flux is almost constant. When we look at the temperature variance $\overline{t^2}$ (Fig. 4a) we find – to our surprise – that the effect of buoyancy is vice versa: $\overline{t^2}$ is larger near the left, hot wall than near the other wall. To understand this, we take a look at the transport equation for $\overline{t^2}$ which reads

$$0 = \underbrace{-2\overline{vt}\frac{\partial\bar{T}}{\partial y}}_{P_{tt}} \underbrace{-\frac{\partial\overline{vt^2}}{\partial y}}_{D^T_{tt}} + \underbrace{\frac{\nu}{Pr}\frac{\partial^2\overline{t^2}}{\partial y\partial y}}_{D^\nu_{tt}} \underbrace{-2\frac{\nu}{Pr}\overline{\frac{\partial t}{\partial x_k}\frac{\partial t}{\partial x_k}}}_{\varepsilon_{tt}} \tag{8}$$

The production term $P_{tt}$ includes the wall-normal heat flux and the temperature gradient $\partial\bar{T}/\partial y$. It was mentioned in connection to Eq. 5 that for the mixed convection case the turbulence near the hot, left wall is decreased, and in order to satisfy Eq. 5 the temperature gradient $\partial\bar{T}/\partial y$ (i.e. the viscous heat flux) must increase. However, the increase in the temperature gradient must be much larger than the decrease in $|\overline{vt}|$, since $1/(Re_\tau Pr) \ll 1$, and this explains why $\overline{t^2}$ is increased via $P_{tt}$ near the left wall, see Fig. 8. Near the right wall the magnitude of $\overline{t^2}$ is similar

to that for the forced convection, and the reason is that the magnitude of the production term $P_{tt}$ is similar for the two cases.

## 4. Conclusions and discussion

DNS of fully developed flow in a vertical channel has been presented. Results from both forced convection and mixed convection are presented. It is found that the effect of the buoyancy on the turbulence can be traced back to the momentum equation. The buoyancy terms in the stress equations are negligible. In forced convection flow the shear stress term $-\overline{uv}$ and the pressure gradient in the momentum equation are in balance in the region where viscous effects are negligible (Fig. 3). This gives a linear (anti-symmetric) shear stress profile. When buoyancy is introduced, the shear stress balances the pressure gradient and the buoyancy term and the result is a strongly modified shear stress. The symmetry is broken and $|\overline{uv}|$ is large near the right, cold wall and small near the left, hot wall (Fig. 3).

As $|\overline{uv}|$ becomes large near the cold wall this generates a large $\overline{u^2}$ through the production $P_{uu} = -2\overline{uv}\partial\bar{U}/\partial y$, and via the pressure-strain term large $\overline{v^2}$ and $\overline{w^2}$ are generated. Also the streamwise heat flux is larger near the cold than near the hot wall. Although the turbulent wall-normal heat flux is lower near the hot wall than near the cold wall, it is fairly constant across the channel. The reason is that it must be constant in the region where viscous effects are negligible in order to satisfy the overall balance of the mean temperature equation. Interestingly enough, the temperature variance $\overline{t^2}$ is *not* larger near the cold wall than near the hot wall (Fig. 4a). The reason is that near the hot wall the mean temperature gradient is larger (to balance the low $|\overline{vt}|$) than near the cold wall. This gives a large production ($-2\overline{vt}\partial\bar{T}/\partial y$) of $\overline{t^2}$ near the hot wall.

**Acknowledgment**

This project was financed by the Swedish Research Council, project number 260-1999-354

## References

1. L. Davidson and S.-H. Peng. Hybrid LES-RANS: A one-equation SGS model combined with a $k-\omega$ model for predicting recirculating flows (to appear). *International Journal for Numerical Methods in Fluids*, 2003.
2. P. Emvin. *The Full Multigrid Method Applied to Turbulent Flow in Ventilated Enclosures Using Structured and Unstructured Grids*. PhD thesis, Dept. of Thermo and Fluid Dynamics, Chalmers University of Technology, Göteborg, 1997.
3. N. Kasagi and O. Iida. Progress in direct numerical simulation of turbulent heat transfer. In *ASME/JSME Joint Thermal Engineering Conference*, San Diego, California, 1999.
4. D. Čuturić. Large-eddy simulation of turbulent channel flow significantly affected by buoyancy. Diploma Thesis 01/07 (can be downloaded from `www.tfd.chalmers/~lada/msc_thesis.html`), Dept. of Thermo and Fluid Dynamics, Chalmers University of Technology, Göteborg, Sweden, 2001.
5. W.K. George and S.P. Capp. A theory for natural convection turbulent boundary layers next to heated vertical surfaces. *International Journal of Heat and Mass Transfer*, 22:813–826, 1979.
6. T. Tsuji and Y. Nagano. Turbulence measurements in a natural convection boundary layer along a vertical surface. *International Journal of Heat and Mass Transfer*, 31(10):2101–2111, 1988.